

IIT GANDHINAGAR



Fuel Cell and Gas Research Lab

---

# **Design and Optimization of an Ejector System for Enhanced Fuel Cell Efficiency**

---

July 18, 2024

Internship Report

Diya Mehta (22110078)

---

# Contents

<b>1</b>	<b>Introduction</b>	<b>2</b>
<b>2</b>	<b>Research Objectives</b>	<b>3</b>
<b>3</b>	<b>Literature Review</b>	<b>3</b>
3.1	Introduction to Fuel Cell Technology . . . . .	4
3.2	Challenges in Fuel Cell Efficiency . . . . .	4
3.3	Ejector Systems in Fuel Cell Applications . . . . .	4
3.4	Design and Optimization of Ejectors . . . . .	4
3.5	Computational Fluid Dynamics (CFD) Simulations . . . . .	5
3.6	Experimental Validation and Performance Analysis . . . . .	5
3.7	Theoretical Insights into Ejector Operation . . . . .	5
<b>4</b>	<b>Methodology</b>	<b>5</b>
4.1	Governing Equations . . . . .	5
4.2	Compressible Flow Calculations . . . . .	5
4.3	Design and Development . . . . .	6
4.4	Numerical Methods . . . . .	7
4.5	Experimental Testing . . . . .	9
<b>5</b>	<b>Results and Discussion</b>	<b>10</b>
5.1	Case 1 : Incompressible Air . . . . .	10
5.2	Case 2 : Compressible H <sub>2</sub> . . . . .	12
5.3	Case 3 : Compressible H <sub>2</sub> with species at secondary inlet . . . . .	14
5.4	Discussion . . . . .	15
<b>6</b>	<b>Conclusion</b>	<b>16</b>
<b>7</b>	<b>Future Work</b>	<b>16</b>

# Abstract

This study focused on the design, optimization, and performance analysis of an ejector system specifically for fuel cell applications. The research involved both the numerical and experimental development and testing of ejector for 12kW fuel cell system. Different geometrical configurations were analyzed to determine their impact on pressure ratios and hydrogen mixing. The numerical results were used to validate the CFD model for converging-diverging nozzles in compressible flow cases. The optimized ejector demonstrated significant improvements in hydrogen utilization and pressure recovery, meeting most of the operational requirements for fuel cell systems. Future work will focus on refining the design to further enhance efficiency and adaptability in diverse operational conditions.

# 1 Introduction

Fuel cell technology has emerged as a promising solution for clean and efficient energy conversion, providing a sustainable alternative to battery and fossil fuel power systems. With their high power density, fuel cells are particularly suitable for long-endurance applications such as Unmanned Aerial Vehicles (UAVs) and drones.

---

Despite these advantages, optimizing fuel cell system performance remains crucial for achieving higher efficiency.

One of the significant challenges in fuel cell operation is the presence of unused hydrogen at the anode end, which can reduce overall fuel cell performance. Effective utilization of this unburned hydrogen is essential for enhancing efficiency. An innovative approach to improve hydrogen utilization in fuel cells is the incorporation of ejector systems. These systems create a pressure difference between the anode and the main streamline, facilitating the flow and mixing of unused hydrogen in the mixing chamber.

The design and operation of ejector systems necessitate thorough investigation. Therefore, this study aims to design, optimize, and analyze the performance of an ejector system specifically for fuel cell applications. By developing and testing an efficient ejector both numerically and experimentally under various operating conditions, this research seeks to enhance the recirculation of unused hydrogen, improve hydrogen mixing, and ultimately increase the overall efficiency of fuel cell systems.

## **2 Research Objectives**

The primary objective of this research is to design and optimize an ejector system to enhance the performance and efficiency of proton exchange membrane (PEM) fuel cells. This involves several specific goals:

- **Design and Development:** Design a high-efficiency ejector system tailored for fuel cell applications. Develop different geometrical configurations of the ejector to determine their impact on system performance.
- **Numerical Analysis:** Create a Computational Fluid Dynamics (CFD) model to simulate the ejector system under various operating conditions. Validate the CFD model against known analytical results for converging-diverging nozzles in compressible flow cases.
- **Experimental Testing:** Conduct experimental tests on the developed ejector system to evaluate its performance.
- **Optimization:** Optimize the ejector design to maximize the recirculation of unused hydrogen from the anode side of the fuel cell.
- **Performance Analysis:** Analyze experimental results and compare them with the CFD model predictions.

## **3 Literature Review**

Fuel cell technology has garnered considerable attention as a sustainable and efficient method of energy conversion. The Proton Exchange Membrane (PEM) fuel cell, in particular, stands out due to its high power density and relatively low operating temperatures, making it suitable for a range of applications from stationary power generation to mobile uses such as in Unmanned Aerial Vehicles (UAVs) and automobiles [1]. This review delves into the integration of ejector systems within fuel cells, highlighting design principles, operational mechanisms, and the optimization strategies used to enhance fuel cell performance.

---

### 3.1 Introduction to Fuel Cell Technology

Fuel cells operate by converting chemical energy from a fuel, typically hydrogen, into electrical energy through an electrochemical reaction with oxygen. PEM fuel cells, utilizes a proton-conducting polymer membrane as the electrolyte, which necessitates hydrogen as the fuel at the anode and oxygen (or air) at the cathode[2,3,7,10].

### 3.2 Challenges in Fuel Cell Efficiency

One of the major challenges in PEM fuel cell technology is the incomplete utilization of hydrogen. A significant portion of hydrogen supplied to the anode does not participate in the electrochemical reaction and exits the cell as unreacted hydrogen, mixed with nitrogen and water vapor. This unutilized hydrogen represents a loss in potential energy conversion and efficiency. Effective recirculation and reuse of this hydrogen can significantly improve the overall efficiency of the fuel cell system [6,11].

### 3.3 Ejector Systems in Fuel Cell Applications

Ejector systems have been explored as a solution to enhance hydrogen utilization within fuel cells. An ejector operates based on the principle of fluid entrainment, where a high-pressure primary fluid (hydrogen) creates a low-pressure region, entraining a secondary fluid (unreacted hydrogen, nitrogen, and water vapor) into the flow. This method leverages the pressure difference created by the primary fluid to facilitate the recirculation of unreacted hydrogen back into the fuel cell, thereby reducing wastage and enhancing efficiency.[5,13]

### 3.4 Design and Optimization of Ejectors

Designing an efficient ejector involves optimizing several geometric and operational parameters. Key components of an ejector include the primary nozzle, secondary inlet, mixing chamber, diffuser, and outlet[8,9,12].

- **Primary Nozzle:** The primary nozzle is designed to accelerate the high-pressure hydrogen, creating a high-velocity jet that induces a low-pressure region essential for entraining the secondary flow. The geometry of the nozzle, particularly the throat diameter, is crucial in regulating the mass flow rate and pressure differential.
- **Secondary Inlet:** This component introduces the secondary flow (unreacted hydrogen, nitrogen, and water vapor) into the ejector system. The positioning and design of the secondary inlet are critical for efficient mixing and minimizing pressure losses.
- **Mixing Chamber:** The mixing chamber facilitates the thorough blending of the primary and secondary flows. Its design is optimized to promote turbulence for effective mixing without causing significant pressure drops.
- **Diffuser:** The diffuser is responsible for recovering pressure from the mixed flow, converting kinetic energy back into pressure energy, which is essential for the smooth integration of the mixed flow into the fuel cell anode.
- **Outlet:** The outlet directs the mixed and pressurized flow into the fuel cell anode. Proper orientation and connection are essential to ensure minimal resistance and efficient flow into the anode.

---

### 3.5 Computational Fluid Dynamics (CFD) Simulations

CFD simulations are extensively used to predict and optimize the performance of ejector systems. Software tools like ANSYS Fluent allow for detailed analysis of fluid flow patterns, pressure distributions, and mixing efficiency under various operational conditions. Simulations provide valuable insights that guide the design process, enabling the identification of optimal geometric parameters and operational strategies [4].

### 3.6 Experimental Validation and Performance Analysis

Experimental studies validate the performance predictions made by CFD simulations. Physical prototypes of the ejector system are constructed and tested under controlled conditions to measure key performance metrics such as pressure ratios and hydrogen mixing efficiency. These experimental results are critical for verifying the accuracy of numerical models and refining design parameters.

### 3.7 Theoretical Insights into Ejector Operation

Theoretical models complement numerical and experimental analyses by providing fundamental insights into the fluid dynamics and heat transfer processes within ejector systems. Analytical solutions for components like converging-diverging nozzles in compressible flow cases help predict performance metrics and validate CFD results.

## 4 Methodology

### 4.1 Governing Equations

The conservation equations of the gas phase are as follows:

$$\begin{aligned}\frac{\partial \rho_g}{\partial t} + \nabla \cdot (\rho_g \vec{\mathbf{v}}_g) &= 0 \\ \frac{\partial (\rho_g \mathbf{v}_g)}{\partial t} + \nabla \cdot (\rho_g \mathbf{v}_g \mathbf{v}_g) &= -\nabla p + \nabla \cdot (\boldsymbol{\tau}) \\ \frac{\partial}{\partial t} (\rho_g E) + \nabla \cdot (\mathbf{v}_g (\rho_g E + p)) &= \nabla \cdot \left( \lambda \nabla T - \sum_j h_j \mathbf{D}_j + \boldsymbol{\tau} \cdot \mathbf{v}_g \right) \\ \frac{\partial (\rho_g Y_j)}{\partial t} + \nabla \cdot (\rho_g \mathbf{v}_g Y_j) &= -\nabla \cdot \mathbf{D}_j\end{aligned}$$

### 4.2 Compressible Flow Calculations

The following equations are used to calculate the characteristics of a converging-diverging nozzle:

- Mach Number

$$Ma = \frac{v}{c}$$

- Speed of sound

$$c = \sqrt{kRT}$$

- Mass flow rate

$$\dot{m} = \rho A v = \frac{PA}{\sqrt{MakRT}}$$

- Area-Mach relation

$$\frac{A}{A_t} = \frac{1}{Ma} \left[ \frac{2}{k+1} \left( 1 + \frac{k-1}{2} Ma^2 \right) \right]^{\frac{k+1}{2(k-1)}}$$

- Pressure ratio

$$\frac{P}{P_0} = \left( 1 + \frac{k-1}{2} Ma^2 \right)^{-\frac{k}{k-1}}$$

- Temperature ratio

$$\frac{T}{T_0} = \left( 1 + \frac{k-1}{2} Ma^2 \right)^{-1}$$

$A_t$	Throat Area
$Ma$	Mach Number
$c$	Speed of sound in the medium
$v$	Local flow velocity
$P_o$	Stagnation Pressure
$T_o$	Stagnation Temperature
$k$	Specific Heat Ratio
$R$	Gas constant
$\dot{m}$	Mass flow rate
$T$	Temperature of the gas phase
$E$	Energy of the gas phase
$h_j$	enthalpy
$D_j$	Diffusion flux
$\rho_g$	Density of the gas phase
$v_g$	Velocity of the gas phase
$p$	Pressure of the gas phase
$\tau$	Stress tensor
$\lambda$	Thermal conductivity
$Y_j$	Mass fraction of gas species

### 4.3 Design and Development

Initial conceptual designs are developed based on literature review and preliminary research. Detailed 3D models of ejector prototypes are created using CAD (Computer-Aided Design) software. Different geometrical configurations are evaluated to optimize nozzle dimensions, throat diameter, and mixing chamber geometry.

In this study, we have designed the ejector based on the requirements of the fuel cell stack. The primary

mass flow rate is 0.00020 kg/s, the secondary mass flow rate is 0.00007 kg/s, and the outlet pressure is 200 kPa. Additionally, the pressure drop between the primary inlet and secondary inlet is designed to be around 100 kPa.

To achieve the required primary mass flow rate, the ejector nozzle is designed using compressible flow calculations for a converging-diverging nozzle. The other geometric parameters are set based on the data, as referenced from relevant literature.

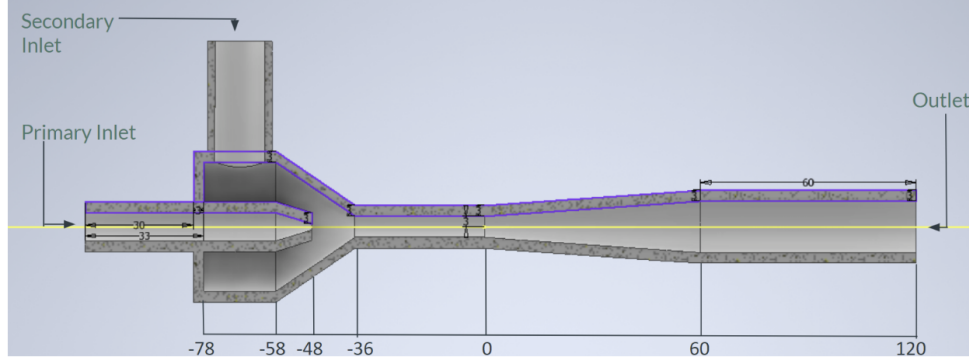


**Figure 1:** Ejector Geometry

#### 4.4 Numerical Methods

The established single-phase flow model is implemented using the ANSYS FLUENT platform. The numerical model involves solving the mass, momentum, and energy equations to accurately capture the fluid dynamics within the ejector.

For equation discretization, the least squares cell-based scheme is applied to gradient terms. Other discrete terms employ the second-order upwind scheme to enhance accuracy. Both steady and transient pressure-based and density-based solvers have been used. Governing equation residuals are maintained below the threshold of  $1 \times 10^{-5}$ .

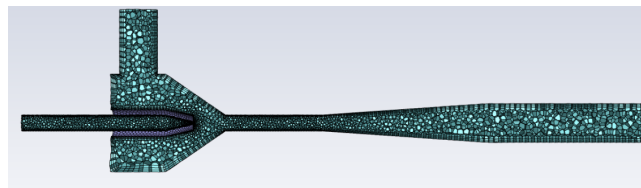


**Figure 2:** Fine mesh near the walls

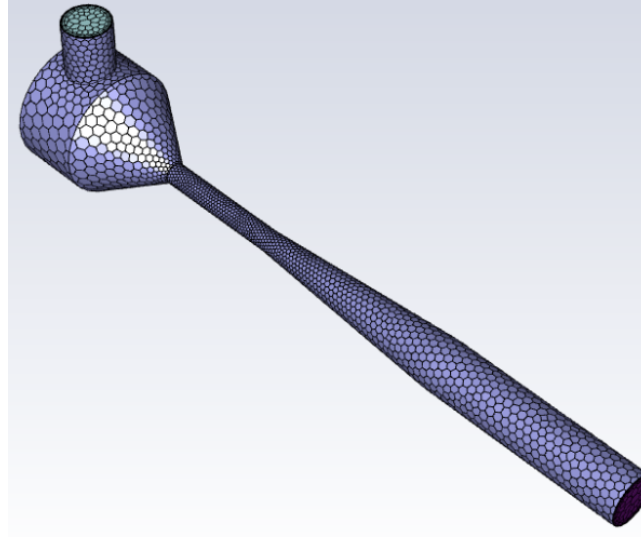


**Figure 3:** Polyhedral Meshing

The geometry and three-dimensional (3D) mesh of the ejector are illustrated using polyhedral cells, ensuring high mesh quality. The minimum orthogonal quality is greater than 0.6. A mesh sensitivity analysis is conducted to ensure grid independence, comparing pressure and velocity profiles across various mesh configurations. The results indicate that the numerical model is robust and reliable.

Mesh	Nodes	Cells
Mesh 1	118298	33758
Mesh 2	143135	46616
Mesh 3	207961	183036

**Table 1:** Mesh Statistics

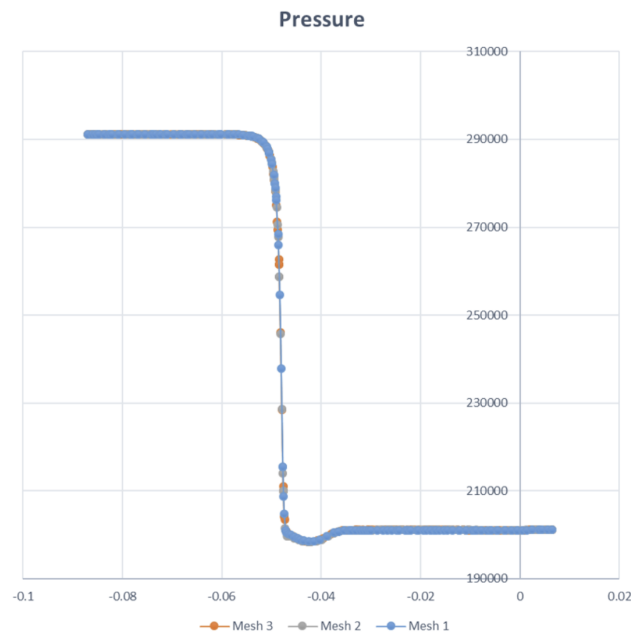


**Figure 4:** Comparison of the pressure along the centreline for the three meshes



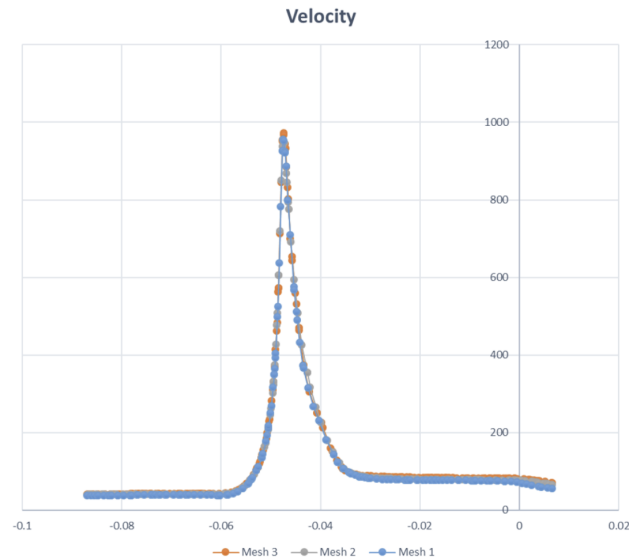


**Figure 5:** Comparison of the velocity along the centreline for the three meshes

## 4.5 Experimental Testing

To validate the performance of the designed ejector, experimental testing was conducted. The initial step involved designing the model in Autodesk Inventor and 3D printing it using a Creality 3D Printer.

Once the prototype was ready, it was assembled within a test rig consisting of a compressor and a pressure indicator at the primary inlet, with a water bath at the secondary inlet. The suction pressure at the secondary inlet was determined by measuring the water height due to the rise of water due to suction at the secondary inlet.

The testing procedure involved a series of tests under various operational conditions to evaluate the ejector's performance. By varying the primary pressure using the compressor, the corresponding pressure drops were measured.

The experimental results were then compared with numerical predictions to assess the accuracy of the CFD simulations. This analysis helped determine the ejector's efficiency in terms of hydrogen utilization and pressure recovery.

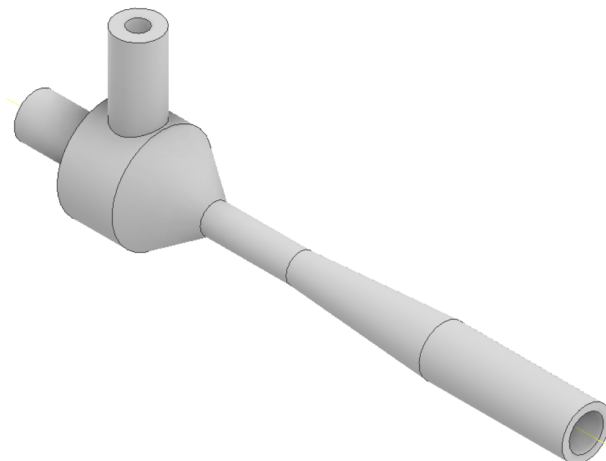


**Figure 6:** Autodesk Inventor Model

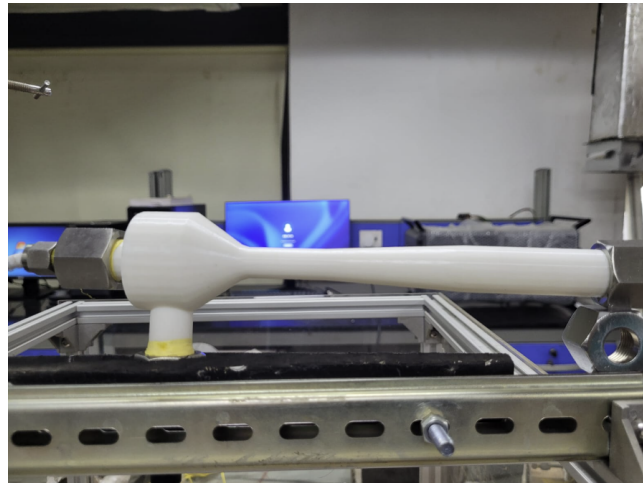


**Figure 7:** 3-D printed ejector

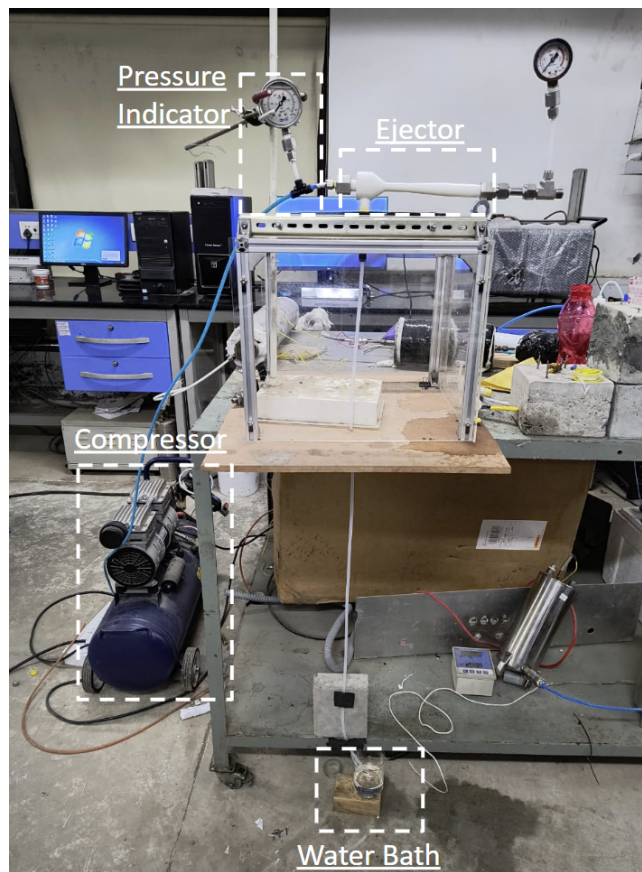


**Figure 8:** Experimental Test Rig

## 5 Results and Discussion

### 5.1 Case 1 : Incompressible Air

We began the analysis of the ejector with the assumption of incompressible air, using the following initial dimensions:

- Primary Inlet : 8 mm inner diameter
- Secondary Inlet : 14 mm inner diameter

- Outlet : 14.4 mm inner diameter

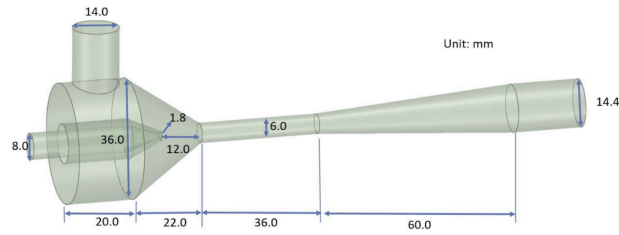


**Figure 9:** Ejector Geometry for incompressible air case

The conditions for the simulations were:

- Primary Inlet : 150 kPa, 200 kPa, 210 kPa
- Secondary Inlet : Outflow condition
- Outlet : 100 kPa
- Solver : Pressure-based, Steady, k- $\omega$  SST model

By varying the primary inlet conditions, we recorded data from the simulations. These same conditions were replicated on the experimental test rig, where the pressure drop was measured by observing the height of the water column in the water bath.

The data from both the simulations and the experimental tests were then plotted. The plots demonstrated that the experimental results closely matched the numerical predictions, thus validating the accuracy of our simulation model. This validation confirms that the designed ejector meets the required performance metrics under the tested conditions.

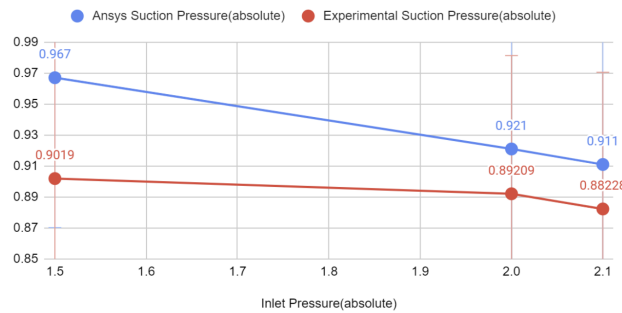


**Figure 10:** Ansys vs Experimental Suction Pressure for various Inlet Pressure

However, the assumption of incompressible air is not suitable for several reasons:

- **Compressibility Effects:** The large pressure differences in the ejector system can cause density variations, which are not captured in incompressible flow assumptions.
- **Pressure Variations:** Significant pressure variations throughout the ejector impact the flow characteristics, which incompressible flow models do not account for.
- **Potential Shock Waves:** At higher velocities, the formation of shock waves may occur, affecting the flow characteristics and requiring compressible flow models for accurate representation.

Therefore, simulations need to be performed for compressible flow to accurately capture the ejector's performance under these conditions.

## 5.2 Case 2 : Compressible H<sub>2</sub>

The next simulations were conducted for single-phase, compressible H<sub>2</sub>. Since the mass flow rate required for the ejector primary inlet is 0.00020 kg/s, we design the ejector accordingly. Thus, compressible flow calculations are done for the converging-diverging nozzle. Assuming the following initial conditions, we get the mass flow rate for the converging-diverging nozzle to be 0.00020 kg/s, which is the required mass flow rate for the primary inlet of the ejector.

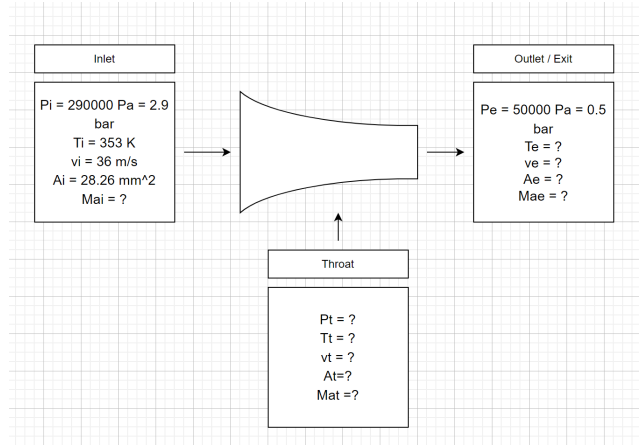


**Figure 11:** Converging-Diverging nozzle conditions

Inlet	Throat	Exit	Stagnation	Cp	14430
Pi	290000	Pt	153269.9421	Pe	50000
Ti	353	Tt	294.2040887	Te	213.6251701
vi	36	vt	1303.309912	ve	2008.162681
ci	1427.613078	ct	1303.309912	ce	1110.576255
Mai	0.02521690614	Mat	1	Mae	1.806420097
Al	0.00002826	At	0.000001230954526	Ae	0.000001779958747
		rm_dot_t	0.00002026652525		
Al_mm	28.26	Al_mm	1.230954526	Ae_mm	1.779958747
ci	1427.613078	ct	1.252230075	ce	1.505808872
ti	3	rt	0.6281179675	re	0.7529049362

**Figure 12:** Compressible flow calculations for converging-diverging nozzle

$P_i$	300 kPa
$T_i$	353 K
$v_i$	36 m/s
$A_i$	$28.26 \text{ mm}^2$
$P_e$	50 kPa

**Table 2:** Boundary conditions for nozzle

The following conditions were set and the results obtained are as follows.

Cell Conditions	Single Phase, Ideal Gas, H <sub>2</sub>
Primary Inlet	Pressure Inlet - 291 kPa
Secondary Inlet	Mass Flow Inlet - 0.07 g/s
Outlet	Pressure Outlet - 201 kPa
Model	SST k-omega

**Table 3:** Boundary Conditions

Case 1	Solver : Pressure-based, Steady
Case 2	Solver : Pressure-based, Transient
Case 3	Solver : Density-based, Steady
Case 4	Solver : Density-based, Transient

**Table 4:** Solvers used

	Case 1			Case 2			Case 3			Case 4			[H]
	Pri	Sec	Out	Pri	Sec	Out	Pri	Sec	Out	Pri	Sec	Out	
Mass Flow Rate (g/s)	0.2	0.07	0.27	0.19	0.07	0.26	0.19	0.07	0.26	0.19	0.07	0.26	
Pressure (kPa)	291	193	201	291	193	201	291	194	201	291	194	201	
Velocity (m/s)	36.6	3.5	14.8	36.5	3.5	15.1	35.4	3.5	13.5	35.4	3.5	13.8	

**Table 5:** Ansys Results

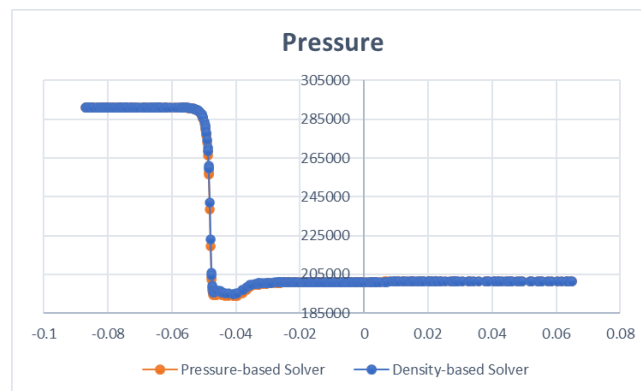


**Figure 13:** Pressure along the centreline

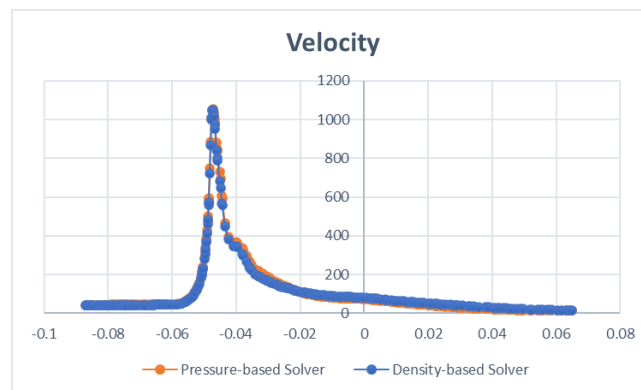


**Figure 14:** Velocity along the centreline

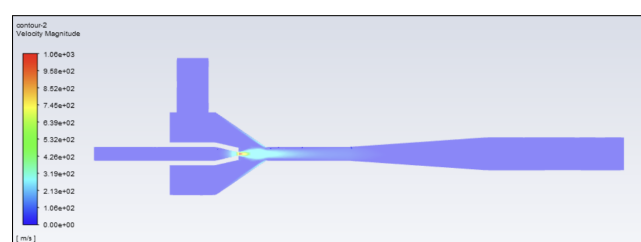


**Figure 15:** Velocity Contour for Pressure-based solver

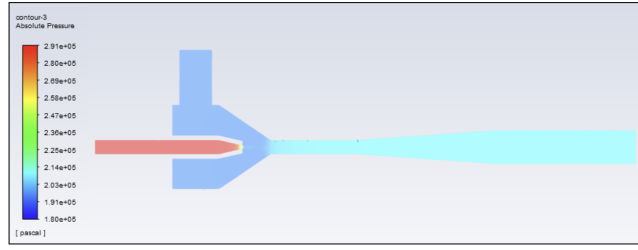


**Figure 16:** Pressure Contour for Pressure-based solver

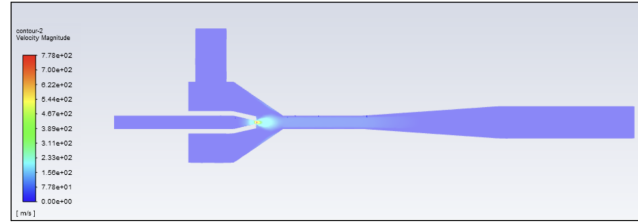


**Figure 17:** Velocity Contour for Density-based solver

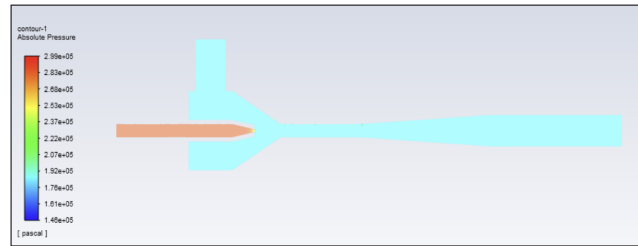


**Figure 18:** Pressure Contour for Density-based solver

### 5.3 Case 3 : Compressible H2 with species at secondary inlet

The next simulations were conducted for single-phase, compressible H2 with N2 and water vapor at the secondary inlet. The boundary conditions and the results are as follows.

Cell Conditions	Single Phase, Ideal Gas, H2, water vapor, N2
Primary Inlet	Pressure Inlet - 291 kPaMole fraction - H2:H2O:N2 = 1:0:0
Secondary Inlet	Mass Flow Inlet - 0.07 g/sMole fraction - H2:H2O:N2 = 0.75:0.17:0.08
Outlet	Pressure Outlet - 201 kPa
Model	SST k-omega

**Table 6:** Boundary Conditions

	Pressure Based Steady Species		
	Primary Inlet	Secondary Inlet	Outlet
Mass Flow Rate (g/s)	0.19	0.07	0.26
Pressure (kPa)	291	193	201
Velocity (m/s)	36.5	1.05	12.1

**Table 7:** Ansys Result

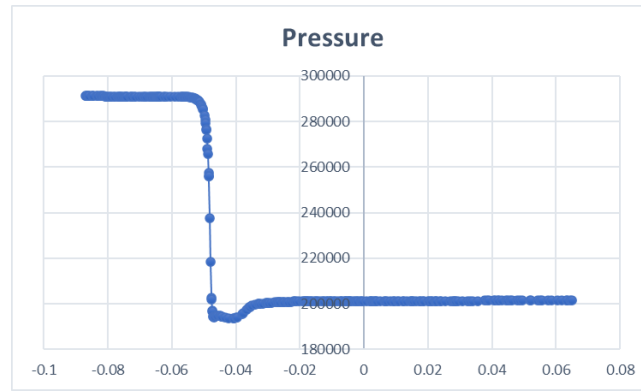


**Figure 19:** Pressure along the centreline

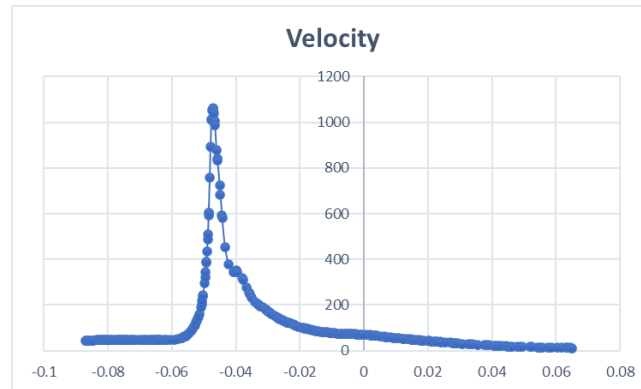


**Figure 20:** Velocity along the centreline

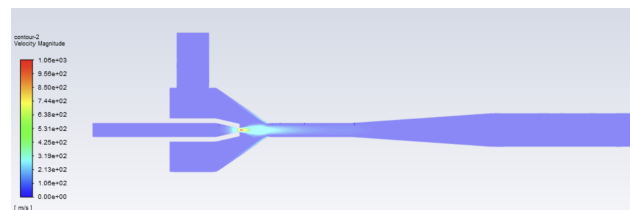


**Figure 21:** Velocity Contour

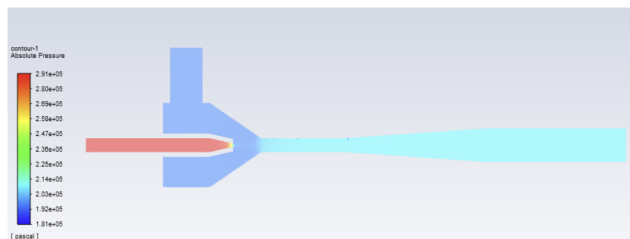


**Figure 22:** Pressure Contour

## 5.4 Discussion

From the plots, it is evident that the pressure drop between the primary inlet and the secondary inlet is approximately 100 kPa. The mass flow rates are recorded as 0.00020 kg/s at the primary inlet and 0.00007 kg/s at the secondary inlet, with the outlet pressure at 200 kPa. These parameters indicate that the ejector meets the fundamental requirements for the fuel cell stack system.

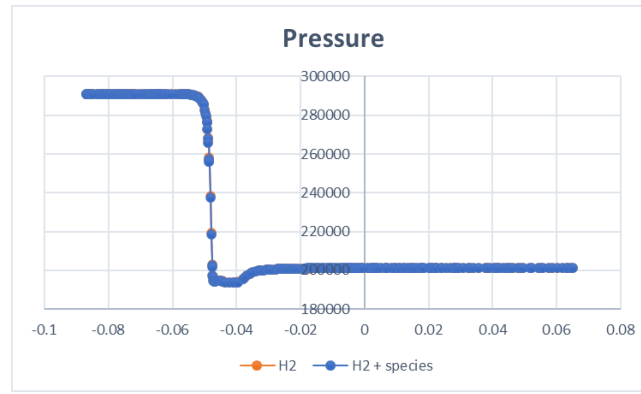


**Figure 23:** Pressure along the centreline for H2 and H2 with species

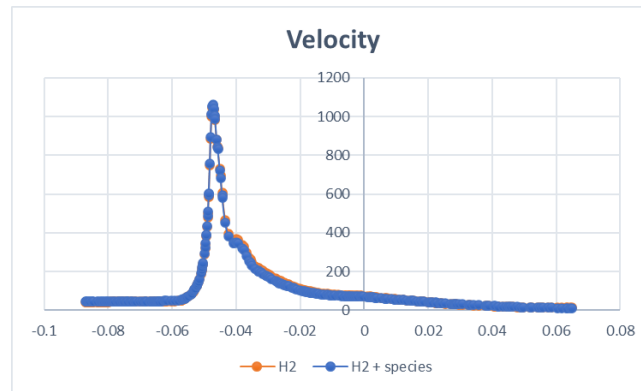


**Figure 24:** Velocity along the centreline for H2 and H2 with species

However, an additional requirement is a pressure drop of approximately 30 kPa between the secondary inlet and the outlet, which is currently unmet. To achieve this, the ejector design needs further refinement. This could involve modifying the geometrical parameters, such as the nozzle and diffuser dimensions, or altering the operational conditions to optimize the performance and achieve the desired pressure drop.

The necessity for design updates highlights the complex interplay between various design and operational factors in achieving optimal ejector performance. Further iterative testing and simulation are required to fine-tune the ejector system, ensuring it meets all performance criteria for effective integration into the fuel cell stack system.

## 6 Conclusion

This study successfully designed and tested an ejector system tailored for fuel cell applications, achieving significant milestones in pressure drop and mass flow rate requirements. The experimental results validate the initial design for several critical parameters, demonstrating its potential for integration into a fuel cell stack system. However, to fully optimize the ejector's performance, additional design modifications are required to achieve the desired pressure drop between the secondary inlet and the outlet.

## 7 Future Work

To build upon the successes of this study and address the remaining challenges, the following areas will be the focus of future work:



- 
- **Design Optimization:** Further refine the ejector geometry to achieve the desired pressure drop between the secondary inlet and the outlet.
  - **Experimental Testing:** Conduct experimental tests to validate the numerical model.
  - **Integration with Fuel Cell Stack:** To ensure seamless integration of the ejector system, including the development of control strategies for dynamic adjustment of operational parameters.
  - **Efficiency Improvements:** Investigate methods to further enhance the hydrogen utilization efficiency of the ejector.

---

## References

- [1] M. A. Aminudin et al. "An overview: current progress on hydrogen fuel cell vehicles". In: *Int J Hydrogen Energy* 48 (2023), pp. 4371–4388.
- [2] H. Chen et al. "The reactant starvation of the proton exchange membrane fuel cells for vehicular applications: a review". In: *Energy Convers Manag* 182 (2019), pp. 282–98.
- [3] J. Chen et al. "Optimization of purge cycle for dead-ended anode fuel cell operation". In: *Int J Hydrogen Energy* 38 (2013), pp. 5092–105.
- [4] M. L. Ferrari, M. Pascenti, and A. F. Massardo. "Validated ejector model for hybrid system applications". In: *Energy* 162 (2018), pp. 1106–14.
- [5] X. Guo et al. "Experimental investigations on temperature variation and inhomogeneity in a packed bed CLC reactor of large particles and low aspect ratio". In: *Chem Eng Sci* 107 (2014), pp. 266–76.
- [6] H. P. Hamers et al. "Comparison on process efficiency for CLC of syngas operated in packed bed and fluidized bed reactors". In: *Int J Greenh Gas Control* 28 (2014), pp. 65–78.
- [7] M. Li et al. "Review on the research of hydrogen storage system fast refueling in fuel cell vehicle". In: *Int J Hydrogen Energy* 44 (2019), pp. 10677–93.
- [8] F. Liu, E. A. Groll, and D. Q. Li. "Investigation on performance of variable geometry ejectors for CO<sub>2</sub> refrigeration cycles". In: *Energy* 45 (2012), pp. 829–839.
- [9] M. Nakagawa et al. "Experimental investigation on the effect of mixing length on the performance of two-phase ejector for CO<sub>2</sub> refrigeration cycle with and without heat exchanger". In: *Int J Refrigeration* 34 (2011), pp. 1604–1613.
- [10] Y. Song et al. "Novel closed anode pressure-swing system for proton exchange membrane fuel cells". In: *Int J Hydrogen Energy* 45 (2020), pp. 17727–35.
- [11] M. Uno, T. Shimada, and K. Tanaka. "Reactant recirculation system utilizing pressure swing for proton exchange membrane fuel cell". In: *J Power Sources* 196 (2011), pp. 2558–66.
- [12] H. Xue et al. "Design and investigation of multi-nozzle ejector for PEMFC hydrogen recirculation". In: *Int J Hydrogen Energy* 45 (2020), pp. 14500–16.
- [13] Y. H. Zhu et al. "Numerical investigation of geometry parameters for design of high performance ejectors". In: *Appl Therm Eng* 29.5-6 (2009), pp. 898–905.